Organic mixed valence compounds with *N*,*N*-dihydrodimethylphenazine redox centres

Marco Holzapfel,[a] Christoph Lambert,*[a] Carola Selinka[b] and Dietmar Stalke[b]

[a] *Institut für Organische Chemie, Julius-Maximilians-Universität Würzburg, Am Hubland, D-97074 Würzburg, Germany. E-mail: lambert@chemie.uni-wuerzburg.de; Fax: +49(0)931/888 4606*

[b] *Institut für Anorganische Chemie, Julius-Maximilians-Universität Würzburg, Am Hubland, D-97074 Würzburg, Germany*

Received (in Cambridge, UK) 8th May 2002, Accepted 9th July 2002
First published as an Advance Article on the web 6th August 2002

The mixed-valence character of four bis(*N*,*N*-dihydrodimethylphenazine) radical cation derivatives with varying π-electron bridges was investigated. The electron transfer (ET) distance within these derivatives varies from *ca.* 12.5 Å for 1,2-bis[2-(5,10-dihydro-5,10-dimethylphenazinyl)]acetylene (**1**) to *ca.* 19.3 Å for 9,10-bis[2-(5,10-dihydro-5,10-dimethylphenazinyl)ethynyl]anthracene (**4**). All radical cation species show intense intervalence charge-transfer (IV-CT) bands in the NIR. The Mulliken–Hush analysis was used to derive the electronic coupling V, which ranges from 310 to 870 cm^{-1}. Comparisons with analogous ET systems in which the dihydrodimethylphenazine redox centres have been replaced by triarylamine units show that the dihydrodimethylphenazine species have a significantly higher internal reorganisation energy associated with the ET. This behaviour is attributed to C–N stretching and C–C ring modes of the dihydrodimethylphenazine units.

Introduction

Organic mixed-valence compounds are useful probes to investigate adiabatic electron transfer (ET) processes.[1–3] The molecules investigated usually consist of two redox centres which are connected by a saturated or unsaturated bridge.[4–11] If these redox centres are identical the ET is degenerate, but also non-degenerate systems are known as well as multidimensional arrangements with more than two redox centres.[12–16] Within the framework of Marcus–Hush theory[17,18] the adiabatic potential energy surface (PES) is governed by two parameters only: the Marcus reorganisation energy λ (consisting of a vibrational and a solvent contribution) and the electronic coupling energy V. While V is mainly associated with the bridge and its connection to the redox centres (orbital overlap), λ is mainly associated with changes of the redox centres' geometry and the solvent orientation upon ET.[9] Organic redox centres with low internal (vibrational) reorganisation energy are quite common (*e.g.* triarylamines[10,15]) while those with high reorganisation energy are rare (*e.g.* hydrazines).[2,19] In this paper we report the syntheses as well as the electrochemical and UV/Vis/NIR characterisation of bis(dihydrodimethylphenazine) radical cations. Structurally similar species based on phenothiazine have been studied by electrochemical[20] and spectroelectrochemical methods.[21] Like phenothiazine, the dihydrodimethylphenazine unit has a butterfly geometry in its neutral state and flattens upon oxidation to the radical cation and dication. In contrast to triarylamines, dihydrodimethylphenazines are more rigid tricyclic systems. Thus, we supposed that this unit possesses a rather high reorganisation energy.

For our investigations we synthesised a set of compounds **1**–**4** that essentially differ in the length of the bridge. For comparison, the phenylene unit in **3** has been replaced by an anthracene unit in **4**. For further comparison, we also investigated the bis(triarylamine) system **5** in which the dihydrodimethylphenazine units have been replaced by triarylamine redox centres.[10,15]

$$\begin{vmatrix} H_{aa} - E & V \\ V & H_{bb} - E \end{vmatrix} = 0 \qquad (1)$$

with $H_{aa} = \lambda(x^2 + Cx^4)/(1 + C)$ and

$$H_{bb} = \lambda((1 - x)^2 + C(1 - x)^4)/(1 + C)$$

$$V = \frac{\mu_{eg}.\tilde{\nu}_{max}}{\Delta\mu_{ab}} \qquad (2)$$

$$\mu_{eg} = 0.09584\sqrt{\frac{\int\varepsilon(\tilde{\nu})\,d\tilde{\nu}}{\tilde{\nu}_{max}}} \qquad (3)$$

$$\tilde{\nu}_{1/2}\,(HTL) = [16\ln(2)k_b\,T\tilde{\nu}_{max}]^{1/2} \qquad (4)$$

$$\Delta\mu_{ab} = \sqrt{\Delta\mu_{eg}^2 + 4\mu_{eg}^2} \qquad \text{with} \qquad \Delta\mu_{eg} = e \times r \qquad (5)$$

Within a two-state model the adiabatic ground and excited state PES of the radical cations $\mathbf{1}^+$–$\mathbf{4}^+$ can be calculated by solving the secular eqn. (1) where quadratic potentials along the ET coordinate x are used for the diabatic states (Fig. 1). These diabatic (noninteracting) states are those in which the hole is localised on the left hand dihydrodimethylphenazine moiety and on the right hand dihydrodimethylphenazine moiety, respectively. The coupling energy V refers to half the splitting of the adiabatic ground and excited state surface at the ET transition state. Excitation from one minimum of the ground state double-well potential to the excited state refers to an optically induced intervalence charge transfer (IV-CT). These absorption bands are usually found in the NIR. The ET parameters V and λ can be extracted from the IV-CT bands by using the Generalised Mulliken–Hush theory[22,23] (eqn. (2)) in which V is derived from the energy $\tilde{\nu}_{max}$ and the transition moment μ_{eg} of the IV-CT band (eqn. (3)) and the diabatic dipole moment difference ($\Delta\mu_{ab}$) associated with the ET. The latter can be calculated by eqn. (5) where the adiabatic dipole moment difference $\Delta\mu_{eg}$ is approximated by the effective ET distance r (eqn. (5)) between the redox centres, although more elaborate methods are known.[24,25] If one starts from quadratic diabatic

DOI: 10.1039/b204392k

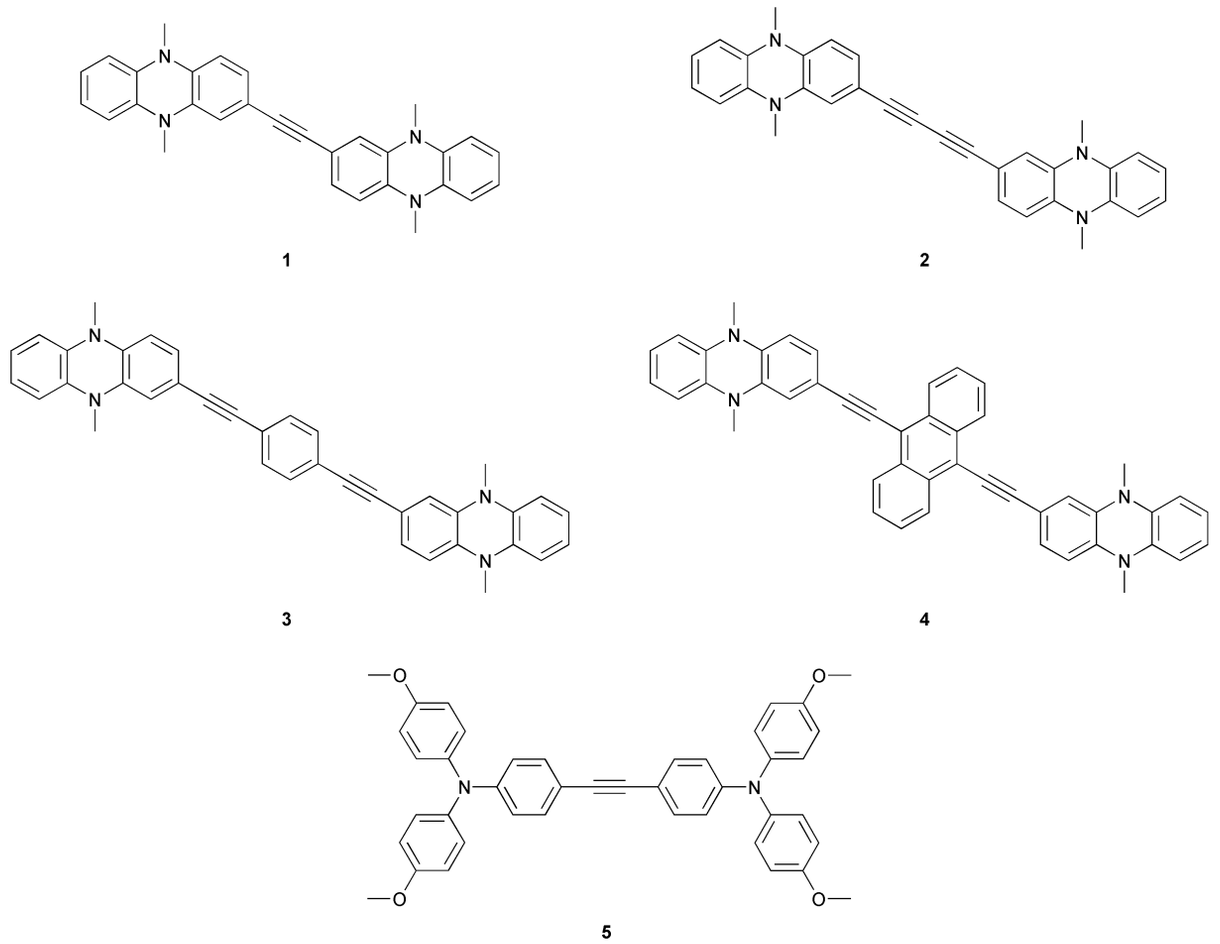

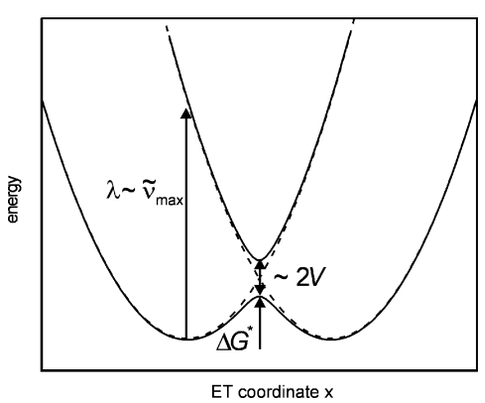

Fig. 1 Diabatic potentials (dashed lines) and adiabatic potentials (solid lines) as derived from the solutions of eqn. (1).

potentials and a Boltzmann-weighted ground state population the resulting IV-CT band is Gaussian-shaped with a distinct band-width at half-height at the so called "high-temperature limit" (eqn. (4)).[18,26] In practice, much broader bands are often observed. Nelsen *et al.* used quartic augmentation[9,27] in order to model a better ground state PES that fits the observed band. This augmentation depends on the parameter *C* and was also used in the present study.

Results and discussion

A. X-Ray structure determination

There have been no investigations of the molecular structure of neutral *N*,*N*-dihydrodimethylphenazine (**DHP**) in the solid state so far. In order to substantiate the geometrical changes which are associated with the oxidation of a **DHP** unit we performed an X-ray structure analysis of neutral **DHP** (see Tables 1 and 2). According to this analysis, the dihedral angle between the two arene planes intersecting along the N,N-axis is 144° (see Fig. 2), which is in good agreement with earlier theoretical calculations.[28] Much in contrast, *N*,*N*-disubstituted

Table 1 Selected bond lengths in **DHP**. The atom labelling is shown in Fig. 2

	DHP/Å	**DHP**$^+$/Å [30]	*Δ*/pm
C(1)–C(6)	1.3877(17)	1.396(5)	0.8
C(1)–N(1)	1.4145(14)	1.372(3)	−4.3
C(1)–C(2)	1.4147(17)	1.409(4)	−0.6
C(2)–C(3)	1.3856(17)	1.397(4)	1.1
C(2)–N(2)	1.4144(14)	1.376(4)	−3.8
C(3)–C(4)	1.3946(17)	1.358(6)	−3.7
C(4)–C(5)	1.3766(19)	1.377(6)	0.0
C(5)–C(6)	1.3976(18)	1.366(5)	−3.2
N(2)–C(8)	1.455(2)	1.474(4)	1.9
N(1)–C(7)	1.457(2)	1.469(4)	1.2

Table 2 Selected bond angles (°) in **DHP**. The atom labelling is shown in Fig. 2

C(6)–C(1)–N(1)	123.93(11)
C(6)–C(1)–C(2)	119.53(10)
N(1)–C(1)–C(2)	116.54(10)
C(3)–C(2)–N(2)	123.89(11)
C(3)–C(2)–C(1)	119.61(10)
C(2)–C(3)–C(4)	120.16(11)
C(5)–C(4)–C(3)	120.39(11)
C(4)–C(5)–C(6)	120.12(11)
C(1)–C(6)–C(5)	120.15(11)
C(1)–N(1)–C(1)	115.22(13)
C(1)–N(1)–C(7)	118.13(7)
C(2)–N(2)–C(2)	114.86(12)
C(2)–N(2)–C(8)	117.95(7)
N(2)–C(2)–C(1)	116.49(10)

Table 3 Half-wave potentials ($E_{1/2}$ *vs.* Fc/Fc^+) and difference between first and second $\Delta E(2–1)$, second and third $\Delta E(3–2)$ and third and fourth $\Delta E(4–3)$ redox process of **1**–**4** from cyclic voltammetry

	$E_{1/2}(1)$/mV	$E_{1/2}(2)$/mV	$\Delta E(2–1)$/mV	$E_{1/2}(3)$/mV	$\Delta E(3–2)$/mV	$E_{1/2}(4)$/mV	$\Delta E(4–3)$/mV
MeCN–0.2 M TBAHFP							
1	−187	−110	77	527	637	622	95
2	−215	−155	60	486	641	555	69
3	−194	−138	56	481	619	537	56
Benzonitrile–0.2 M TBATFB							
1	−186	−94	92				
2	−224	−142	82				
3	−226	−180	46				
4	−218	−159	59				

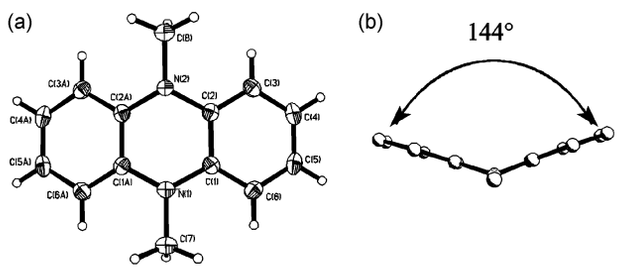

Fig. 2 X-Ray structure of neutral **DHP**: a) view from top, b) view along the Me–N ⋯ N–Me vector.

phenazinium radical cations have been extensively studied in CT-complexes with electron acceptors. The dihedral angle around the N,N-axis of $\mathbf{DHP}^+$ depends on the counteranion. The cations are found to be nearly planar with dihedral angles varying between 180° with tetrafluorotetracyanoquinodimethane $TCNQF_4^-$ [29] or pentamethoxycarbonylcyclopentadienide [30] and 165.5° with I_3^- [31] as the counteranion. There are also significant changes in C–C and C–N bond lengths between neutral **DHP** and $\mathbf{DHP}^+$,[30] up to 4 pm, see Table 1. This contrasts with the behaviour of triphenylamine where the only significant changes upon oxidation concern the dihedral angles between the phenyl rings.[32] Thus, we expect that high frequency C–N and C–C stretching modes are involved in the ET process in **DHP** derived systems while these are less important for triarylamine species.

B. Synthesis

The important intermediate for the synthesis of molecules **1**–**4** is 2-bromophenazine (**7**). Because we were unable to reach the yields for **7** reported in the literature,[33] we developed a new synthetic route to **7** which gave better yields in our hands: 4-bromo-1,2-benzoquinone (**6**) was coupled with an excess of 1,2-phenylenediamine and a catalytic amount of hydrochloric acid in ethanol under reflux. Subsequently, the resulting phenazine **7** was reduced with sodium dithionite according to a similar method developed by Sugimoto *et al.*[34] The intermediate dihydrophenazine was susceptible to oxidation and, therefore, was immediately deprotonated by two equivalents of *n*-BuLi. After the addition of a large excess of MeI we obtained stable 2-bromo-5,10-dihydro-5,10-dimethylphenazine (**8**). Following a procedure published by Hundertmarck *et al.*,[35] we synthesized 2-trimethylsilylethynyl-5,10-dihydro-5,10-dimethylphenazine (**9**) by palladium-catalysed Hagihara coupling of **8** and trimethylsilylacetylene (TMSA) with $P(t\text{-}Bu)_3$ as the ligand. Finally, TBAF was used to remove the trimethylsilyl group in THF to get 2-ethynyl-5,10-dihydro-5,10-dimethylphenazine (**10**) in high yield (see Scheme 1).

The three derivatives **1**, **3** and **4** were synthesized by coupling **10** with either **8**, 1,4-diiodobenzene or 9,10-dibromoanthracene under the palladium-catalysed Hagihara conditions mentioned above. The butadiyne **2** was synthesized by copper-catalysed homo coupling under Glaser–Eglington conditions of the ethynylphenazine **10**.

Compounds **1**–**4** are sparingly soluble in all common organic solvents. Best dissolving properties were found in benzonitrile, which, therefore, was used as the solvent for further electrochemical and spectroscopic investigations.

C. Electrochemical and UV/Vis/NIR spectroscopic properties

Electrochemistry. All compounds **1**–**4** show four reversible oxidation waves in the cyclic voltammograms (CVs) in acetonitrile–0.2 M tetrabutylammonium hexafluorophosphate (TBAHFP) solutions (see Fig. 3). Due to the small redox

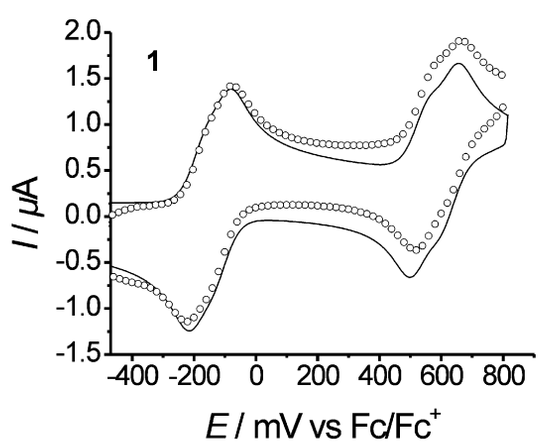

Fig. 3 Cyclic voltammogram of **1** in MeCN–0.2 M TBAHFP; $v = 50$ mV s^{-1}; —— CV-simulation, ◦ CV-measurement.

potential splitting ΔE of the first and second and the third and fourth wave, respectively, the half-wave potentials were obtained by digital simulation of the CVs with DigiSim 3.03.[36] Because of the low concentration of **4** in acetonitrile and, consequently, the very low Faradaic *vs.* capacitive currents, a digital simulation could not be carried out. With solvents such as dichloromethane or benzonitrile the solubility is much better, but adsorption phenomena were observed at the third and the fourth oxidation waves.

As one expects, the closer the distance between the redox centres is, the larger is the redox potential splitting $\Delta E(2–1)$ and $\Delta E(4–3)$, respectively (see Table 3). Even for the compound with the largest distance of the redox centres (**3**) the redox potential splitting $\Delta E(2–1)$ and $\Delta E(4–3)$ is 56 mV. Although these splittings are quite small, they are still larger than 35.6 mV, the statistical value of two completely separated redox centres. These splittings point to a significant electronic coupling of the two redox centres.

Further cyclovoltammetric investigations were carried out in benzonitrile–0.2 M tetrabutylammonium tetrafluoroborate

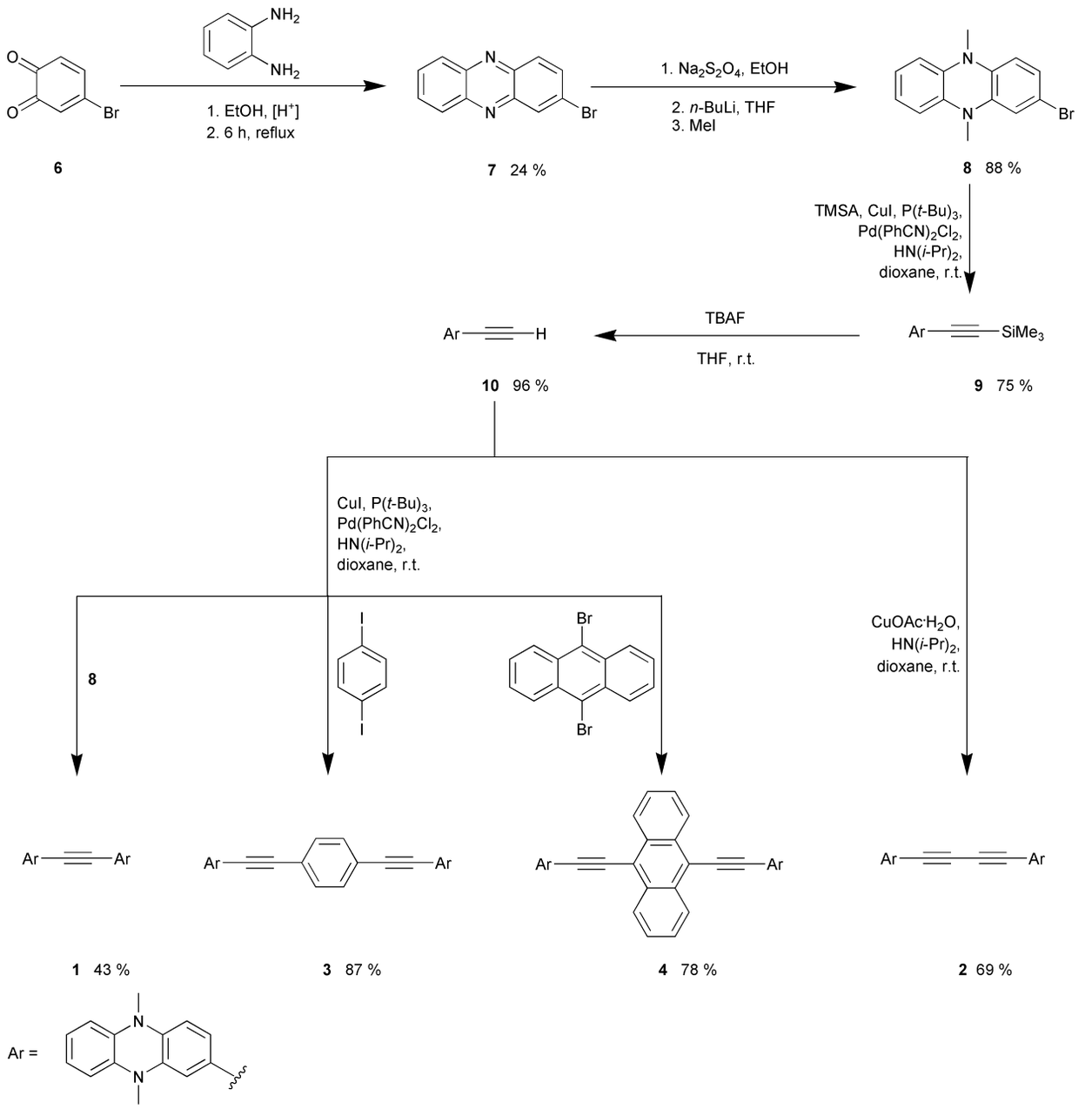

6 **7** 24 % **8** 88 % **10** 96 % **9** 75 % **1** 43 % **3** 87 % **4** 78 % **2** 69 %

Scheme 1

(TBATFB) solutions (see Table 3). Due to the adsorption effects already mentioned, only the first and the second oxidation waves of compounds **1**–**4** are reversible (see Fig. 4). The trend of the potential splittings in benzonitrile is the same as in acetonitrile: with increasing chain length of the spacer $\Delta E(2–1)$ decreases. For compounds **1** and **2** $\Delta E(2–1)$ is distinctly larger in acetonitrile, however, for compound **3** it is larger in benzonitrile. Although **3** and **4** do not differ in the distance of the redox centres, but only in the type of the spacer, the potential splitting of compound **3** is somewhat smaller than that of **4**. This might be due to a stronger delocalisation of the nitrogen lone-pair electrons into the anthracene bridge, which results in a stronger communication between the redox centres.

UV/Vis/NIR spectroscopic properties. The UV/Vis/NIR spectroscopic properties of the bis(dihydrophenazines) **1**–**4** were investigated in benzonitrile (see Fig. 5). The neutral compounds **1**–**3** have an intense absorption band at ~22000–24000 cm^{-1}. Owing to the electron acceptor character of anthracene, the corresponding band of **4** is shifted to lower energy at ~18300 cm^{-1}. This supports our foregoing assumption of stronger N-lone-pair delocalisation into the anthracene bridge.

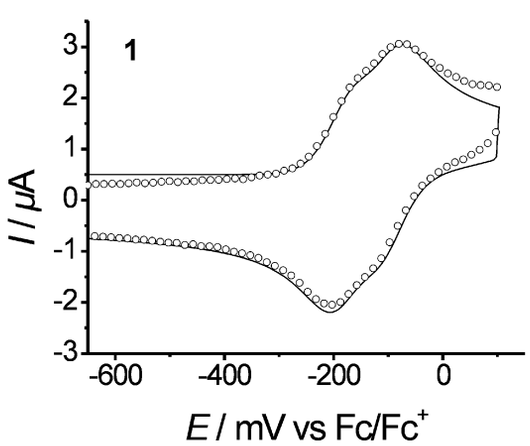

Fig. 4 Cyclic voltammogram of **1** in benzonitrile–0.2 M TBATFB; $v = 250$ mV s^{-1}; —— CV-simulation, ◦ CV-measurement.

Oxidation to the monocation and the dication, respectively, was performed by titration with a diluted $SbCl_5$–benzonitrile solution. Further oxidation to the tri- and tetracation could not

Table 4 Band shape data of the IV-CT band of $\mathbf{1}^+$–$\mathbf{4}^+$ in benzonitrile at 298 K

	$\tilde{\nu}_{max}$/cm^{-1} [a]	ε^+/M^{-1} cm^{-1} [b]	$\tilde{\nu}_{1/2}$ (Fit)/cm^{-1} [c]	$\tilde{\nu}_{1/2}$ (HTL)/cm^{-1}
$\mathbf{1}^+$	8170	4960	6790	4330
$\mathbf{2}^+$	9010	3130	6940	4550
$\mathbf{4}^+$	8800	2240	4670	4500
$\mathbf{5}^+$	6560	10100	4200	3880

[a] ± 100 cm^{-1}. [b] ± 100 M^{-1} cm^{-1}. [c] ± 100 cm^{-1}.

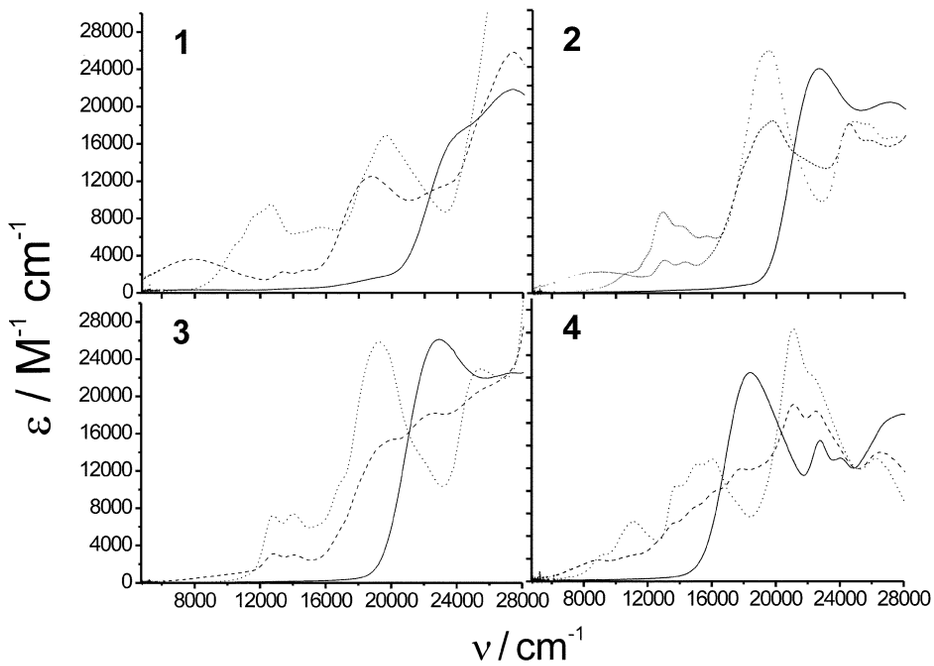

Fig. 5 UV/Vis/NIR spectra of neutral compounds (solid lines), radical cations (dashed lines) and dications (dotted lines) in benzonitrile.

be achieved, although the redox potentials of antimony halides are ≤1045 mV *vs.* Fc/Fc$^+$ which should be sufficiently high.[37] For all compounds a broad absorption band rises at ~5000–11000 cm^{-1} upon oxidation to the monoradical cation, which again decreases at further oxidation to the dication. We assign this absorption to an optically induced IV-CT process in which a hole is transferred from a radical cation centre to a neutral redox centre. The IV-CT bands of $\mathbf{1}^+$–$\mathbf{4}^+$ are less intense (*ca.* 2000–5000 M^{-1} cm^{-1}) than those of the corresponding triarylamine redox systems (*ca.* 0.5–3 × 10^4 M^{-1} cm^{-1}).[10] In the monoradical cations $\mathbf{1}^+$–$\mathbf{4}^+$ a structured band is found at *ca.* 10000–17000 cm^{-1} and a very intense band at *ca.* 17000–24000 cm^{-1}. The dications also show the same two absorption bands but with higher intensity. These absorption bands are typical of dihydrophenazine radical cations and can be assigned to HOMO → SOMO and HOMO-1/HOMO-2 → SOMO-transitions, respectively.[38]

The IV-CT bands for $\mathbf{1}^+$, $\mathbf{2}^+$ and $\mathbf{4}^+$ overlap to some extent with adjacent radical bands but the peak maximum and the low-energy side are clearly visible and should be unaffected by overlap. Therefore, we modelled the PES resulting from a numerical solution of eqn. (1) by adjusting C and λ in order to get the best fit with the observed IV-CT band at the low-energy side and around the maximum (see Fig. 6 and Table 4). For $\mathbf{4}^+$ the fit at the low-energy side is less satisfactory because of somewhat stronger band overlap with adjacent bands, which originate from excitations into the bridge.[39,40] Therefore, the values derived from the fit of $\mathbf{4}^+$ are considered to be less reliable. In the case of $\mathbf{3}^+$, no reasonably accurate fit was possible. The C and λ parameters resulting from all fits are collected in Table 5. The fitted IV-CT bands of $\mathbf{1}^+$ and $\mathbf{2}^+$ are much broader than the theoretical values ($\tilde{\nu}_{1/2}$ (HTL)) at the high-temperature limit expected from simple Marcus–Hush theory using quadratic potentials (C = 0) (see Table 4).[18] One possible physical interpretation of this broadness is the contribution of high-energy vibrations to the ET.[26] Indeed, in the X-ray structure of **DHP** and $\mathbf{DHP}^+$ we found significant deviations between C–N and C–C bond lengths. According to preliminary DFT computations of **DHP** on the B3LYP/6-31G* level, these differences are associated with high-energy C–N and C–C stretching vibrations in the 1070–1120, 1300–1420 and 1500–1670 cm^{-1} region and support the assumption of a higher internal reorganisation energy compared to triarylamine-based systems (*e.g.* $\mathbf{5}^+$) where C–C and C–N bond length differences are much smaller[32] and for which the observed band is only slightly broader than $\tilde{\nu}_{1/2}$ (HTL).[10]

Table 5 N,N-Distance r, transition moment μ_{eg}, coupling energy V and the PES parameters: thermal barrier ΔG^*, reorganisation energy λ and asymmetry parameter C for $\mathbf{1}^+$, $\mathbf{2}^+$, $\mathbf{4}^+$ and $\mathbf{5}^+$ in benzonitrile at 298 K

	r/Å	μ_{eg}/D	V/cm^{-1}	ΔG^*/cm^{-1}	λ/cm^{-1}	C
$\mathbf{1}^+$	12.5	6.5 ± 0.2	870 ± 50	910 ± 100	8500 ± 100	0.7
$\mathbf{2}^+$	15.0	4.9 ± 0.2	600 ± 30	1310 ± 100	9200 ± 100	0.6
$\mathbf{4}^+$	19.3	3.3 ± 0.1	310 ± 20	1880 ± 100	8700 ± 100	0.1
$\mathbf{5}^+$	12.5	9.4 ± 0.2	980 ± 50	740 ± 100	6600 ± 100	0.1

For the evaluation of the electronic coupling V, the effective ET distance r is needed. We approximated this distance by the AM1 calculated N,N-distance belonging to two different dihydrophenazines separated by the corresponding spacer. The transition moment μ_{eg} was calculated by integration of the IV-CT band (eqn. (3)) and the electronic coupling V was evaluated by eqn. (2). We obtained values between 310 cm^{-1} ($\mathbf{4}^+$) and

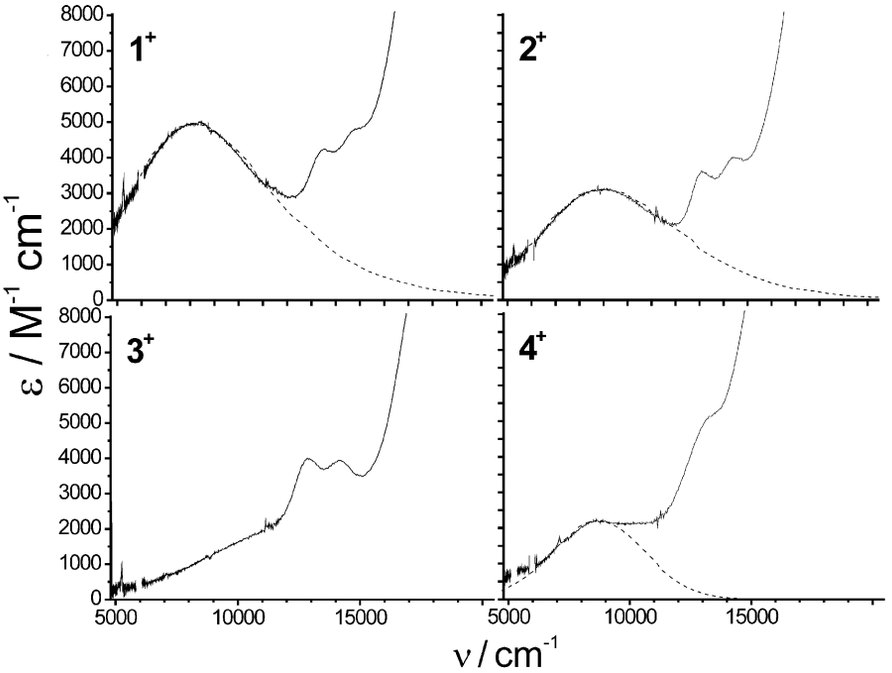

Fig. 6 IV-CT bands of $\mathbf{1}^+$–$\mathbf{4}^+$ (solid lines) in benzonitrile and fits (dotted lines) derived from PES using quartic augmented quadratic potentials.

870 cm^{-1} ($\mathbf{1}^+$). For comparison with bis(dihydrophenazine) $\mathbf{1}^+$, we also investigated the triarylamine system bis{4-[*N*,*N*-bis-(4-methoxyphenyl)amino]phenyl}acetylene radical cation ($\mathbf{5}^+$), which has the same bridge.

The values for V of $\mathbf{1}^+$ (870 cm^{-1}) and of $\mathbf{5}^+$ (980 cm^{-1}) differ only slightly, the one of $\mathbf{5}^+$ being *ca.* 13% larger. The couplings V of $\mathbf{1}^+$, $\mathbf{2}^+$, $\mathbf{4}^+$ and $\mathbf{5}^+$ are comparable to inorganic mixed-valence systems, which usually have somewhat smaller couplings at the same effective ET distance.[41] A plot of ln (V) *vs.* the number of bonds − 1 (n − 1) between the two nitrogen atoms is linear which indicates a superexchange ET mechanism (Fig. 7).[18]

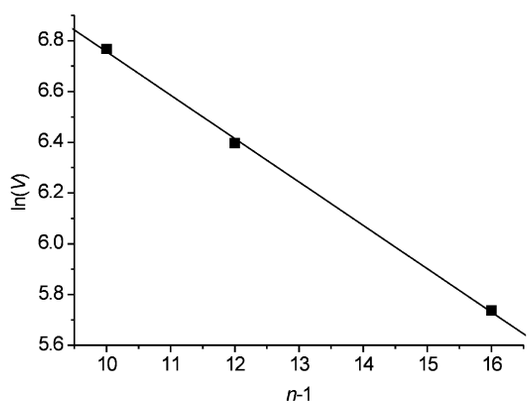

Fig. 7 Correlation of ln (V) of $\mathbf{1}^+$–$\mathbf{3}^+$ *vs.* distance parameter n − 1.

The slope of the correlation (−0.17) is very similar to that of an analogous series of bis(triarylamine) systems (−0.16).[10]

Compounds **3** and **4** just differ in the size of the π-bridge, but not in the distance separating the redox centres. Unfortunately, the strong band overlap of the IV-CT band in $\mathbf{3}^+$ precludes the determination of V and that of $\mathbf{4}^+$ also is relatively uncertain. However, significant differences between the NIR bands of $\mathbf{3}^+$ and $\mathbf{4}^+$ are obvious which might be due to the participation of bridge state bands owing to the low energy of anthracene-oxidised states.[39,40]

Owing to the low solubility of **1**–**4** in organic solvents and due to stability problems we were unable to measure the IV-CT bands of the corresponding cations in solvents other than benzonitrile. Therefore, the separation of the total reorganisation energy λ into a solvent and into an internal contribution was impossible. Nonetheless, because of similar size of the redox centres and equal N,N-distance we estimate the solvent reorganisation energy to be very similar for $\mathbf{1}^+$ and $\mathbf{5}^+$. Thus, the difference of the total reorganisation energy of the dihydrophenazine derivative $\mathbf{1}^+$ and of the triarylamine species $\mathbf{5}^+$ (*ca.* 2000 cm^{-1}, see Table 5) can mainly be attributed to the internal part. We explain the higher internal reorganisation energy of $\mathbf{1}^+$ by the higher-energy C–N and ring C–C modes *vs.* the lower-energy phenyl torsional modes of the triarylamine systems.

Conclusions

The mixed-valence character of four bis(*N*,*N*-dihydrodimethylphenazine) radical cation derivatives with varying π-electron bridges was investigated. The electron transfer (ET) distance within these derivatives varies from *ca.* 12.5 Å (**1**) to *ca.* 19.3 Å (**3**). All radical cation species show intense intervalence charge-transfer (IV-CT) bands in the NIR which were used to derive the electronic coupling V. The linear correlation between ln (V) and the number of bonds separating the nitrogen atoms of the redox centres gives clear evidence for a superexchange ET pathway. Comparison with analogous ET systems in which the dihydrodimethylphenazine redox centres have been replaced by triarylamine units shows that both systems have a very similar electronic coupling V while the dihydrodimethylphenazine species have significantly higher internal reorganisation energy associated with the ET which results in a somewhat higher ET barrier ΔG^* for $\mathbf{1}^+$ *vs.* the triarylamine system $\mathbf{5}^+$. This behaviour is attributed to C–N and C–C stretching modes of the dihydrodimethylphenazine units.

In conclusion, we were able to show that dihydrodimethylphenazine is a versatile redox system, which can be used to build up organic mixed-valence compounds. Systems based on these mixed-valence species might be used in hole-conducting materials for optoelectronic or electrochromic applications.[42,43]

Experimental

Synthesis

Commercial grade reagents were used without further purification. Solvents were purified, dried and degassed following

standard procedures. All air-sensitive manipulations were carried out using flame dried glassware applying Schlenk techniques under nitrogen inert gas atmosphere. *J* values are given in Hz. PE = petroleum ether.

2-Bromophenazine 7. 4-Bromo-1,2-benzoquinone (3.56 g; 18.8 mmol) and 1,2-phenylenediamine (2.03 g; 18.8 mmol) were dissolved in ethanol (180 ml). A catalytic amount of hydrochloric acid was added to the dark red solution which was refluxed for 6 hours. The solvent was removed *in vacuo* and the residue was purified by flash chromatography (PE : CH_2Cl_2 2 : 1). Recrystallisation from ethanol afforded 1.14 g (24%) of yellow crystals, mp 149 °C (lit.:[33] 149–150 °C). δ_H(250 MHz, [D_1]chloroform) 8.42 (1 H, d, $^4J_{HH}$ 1.83, arom. H), 8.24–8.16 (2 H, arom. H), 8.08 (1 H, d, $^3J_{HH}$ 9.15, arom. H), 7.90–7.80 (3 H, arom. H); δ_C(63 MHz, [D_1]chloroform) 143.6, 143.5, 143.4, 141.9, 134.2, 131.6, 131.2, 130.8, 129.7, 129.6, 124.9.

2-Bromo-5,10-dihydro-5,10-dimethylphenazine 8. A solution of sodium dithionite (14.2 g; 81.6 mmol) in water (140 ml) was added to a boiling solution of **7** (2.00 g; 7.72 mmol) in ethanol (40 ml). The green suspension was refluxed until the reaction mixture became colourless. The precipitate was filtered off and dried *in vacuo* which gave 1.95 g (97%) of a colourless powder. ν_{max}(KBr)/cm^{-1} 3371 (N–H), 3305 (N–H). *n*-BuLi (1.92 ml of a 1.6 M solution in hexanes; 3.07 mmol) was added drop by drop to a solution of the dried intermediate (400 mg; 1.53 mmol) in THF at −78 °C. The reaction mixture was stirred for 30 minutes and methyl iodide (1.92 ml; 30.8 mmol) was added. The mixture was allowed to warm up and was stirred for another 20 minutes. Finally, the solvent was removed *in vacuo* and the residue was purified by chromatography on alumina (neutral, activity 5, PE). The crude product was precipitated by dropping a CH_2Cl_2 solution into MeOH, which gave 390 mg (88%) of colourless crystals, mp 104–106 °C (Found: C, 57.93; H, 4.50; N, 9.72. Calc. for $C_{14}H_{13}N_2Br$: C, 58.15; H, 4.53; N, 9.69%); δ_H(400 MHz, [D_6]benzene) 6.82 (1 H, dd, $^4J_{HH}$ 1.64, $^3J_{HH}$ 8.20, arom. H), 6.72–6.32 (2 H, arom. H), 6.32 (1 H, d, $^4J_{HH}$ 2.04, arom. H), 6.12–6.00 (2 H, arom. H), 5.73 (1 H, d, $^3J_{HH}$ 8.36, arom. H), 2.32 (3 H, s, –CH_3), 2.23 (3 H, s, –CH_3); δ_C(101 MHz, [D_6]benzene) 124.5, 122.6, 122.5, 115.0, 114.8, 112.5, 112.1, 111.9, 31.6, 31.5, the missing four ^{13}C-NMR signals are superimposed by the solvent signal. *m*/*z* 288 (M^+, 57%), 273 ($M^+ - CH_3$, 100%).

2-Trimethylsilylethynyl-5,10-dihydro-5,10-dimethylphenazine 9. $Pd(PhCN)_2Cl_2$ (7.96 mg; 20.8 μmol), **8** (200 mg; 0.692 mmol), Cu(I)I (2.63 mg; 13.8 μmol), P(*t*-Bu)$_3$ (126 μl of a 0.33 M solution in hexane; 41.6 μmol), diisopropylamine (117 μl; 0.832 mmol) and trimethylsilylacetylene (118 μl; 0.829 mmol) were dissolved in dioxane (1 ml) and stirred for 2 d at RT. The solvent was removed *in vacuo*. The residue was purified by chromatography on alumina (neutral, activity 5, PE) and the oily product was dissolved in a little CH_2Cl_2 and dropped into MeOH. The solvent was removed under reduced pressure. Recrystallisation from MeOH afforded 160 mg (75%) of beige crystals, which were dried *in vacuo*, mp 106–107 °C. δ_H(250 MHz, [D_6]benzene) 7.08 (1 H, dd, $^4J_{HH}$ 1.53, $^3J_{HH}$ 8.09, arom. H), 6.71–6.62 (2 H, arom. H), 6.49 (1 H, d, $^4J_{HH}$ 1.53, arom. H), 6.10–5.98 (2 H, arom. H), 5.83 (1 H, d, $^3J_{HH}$ 7.95, arom. H), 2.31 (3 H, s, –CH_3), 2.27 (3 H, s, –CH_3); 0.32 (9 H, s, –(CH_3)$_3$); δ_C(63 MHz, [D_6]benzene) 139.9, 138.7, 138.5, 138.2, 126.5, 122.0, 121.6, 116.0, 114.1, 111.2; 111.2, 110.6, 107.7, 107.4, 31.5, 31.3, 0.3; *m*/*z* 306 (M^+, 65%), 291 ($M^+ - CH_3$, 100%); MS (EI, 70 eV, high resolution): *m*/*z* found: 306.1549, calc. for $C_{16}H_{14}N_2$: 306.1552.

2-Ethynyl-5,10-dihydro-5,10-dimethylphenazine 10. Tetrabutylammonium fluoride (630 μl of a 1 M solution in THF; 0.630 mmol) was added to a solution of **9** (192 mg; 0.626 mmol) in THF (1.6 ml) and stirred for 1 hour at RT. The solvent was removed *in vacuo*. The residue was dissolved in CH_2Cl_2 and washed with water (3 × 20 ml). The organic layer was dried over Na_2SO_4 and the solvent was removed under reduced pressure which gave 140 mg (96%) of a green powder, mp 69–70 °C (Found: C, 82.38; H, 5.78; N, 11.74. Calc. for $C_{16}H_{14}N_2$: C, 82.02; H, 6.02; N, 11.96%); δ_H(250 MHz, [D_6]benzene) 7.00 (1 H, dd, $^4J_{HH}$ 1.53, $^3J_{HH}$ 8.23, arom. H), 6.72–6.61 (2 H, arom. H), 6.41 (1 H, d, $^4J_{HH}$ 1.53, arom. H), 6.12–5.98 (2 H, arom. H), 5.82 (1 H, d, $^3J_{HH}$ 8.23, arom. H), 4.27 (1 H, s, ≡C*H*), 2.84 (3 H, s, –CH_3), 2.79 (3 H, s, –CH_3); δ_C(63 MHz, [D_6]benzene) 140.0, 138.8, 138.5, 138.2, 126.5, 122.0, 121.6, 115.0, 114.2, 111.3, 111.3, 110.7, 85.1, 76.2, 31.6, 31.4.

1,2-Bis[2-(5,10-dihydro-5,10-dimethylphenazinyl)]acetylene 1. $Pd(PhCN)_2Cl_2$ (6.88 mg; 17.9 μmol), Cu(I)I (2.28 mg, 12.0 μmol), P(*t*-Bu)$_3$ (109 μl of a 0.33 M solution in hexane; 36.0 μmol), diisopropylamine (101 μl; 0.719 mmol), **8** (173 mg; 0.598 mmol) and **10** (140 mg; 0.600 mmol) were dissolved in dioxane (1 ml) and stirred for 60 hours at RT. The solvent was removed *in vacuo*. The residue was purified by chromatography on alumina (neutral, activity 5, gradient PE ⟶ PE : CH_2Cl_2 1 : 1). The crude product was purified by micro extraction with CH_2Cl_2 which gave 113 mg (43%) of a light red powder, mp 277–278 °C (Found: C, 81.72%; H, 5.95; N, 12.45. Calc. for $C_{30}H_{26}N_4$: C, 81.42; H, 5.92; N, 12.66%); δ_H(250 MHz, [D_6]benzene) 7.00 (2 H, dd, $^4J_{HH}$ 1.53, $^3J_{HH}$ 8.24, arom. H), 6.74–6.61 (4 H, arom. H), 6.64 (2 H, d, $^4J_{HH}$ 1.53, arom. H), 6.15–6.03 (4 H, arom. H), 5.96 (2 H, d, $^3J_{HH}$ 8.25, arom. H), 2.39 (6 H, s, –CH_3), 2.38 (6 H, s, –CH_3); *m*/*z* 442 (M^+, 100), 206 ($M^{2+} - 2\ CH_3$, 96%).

1,4-Bis[2-(5,10-dihydro-5,10-dimethylphenazinyl)]buta-1,3-diyne 2. Copper(II) acetate monohydrate (140 mg; 0.701 mmol), diisopropylamine (100 μl; 0.712 mmol) and **10** (160 mg; 0.683 mmol) were dissolved in dioxane (2 ml) and stirred for 1 d at RT. The solvent was removed *in vacuo* and the residue was dissolved in CH_2Cl_2 (30 ml) and washed with water (3 × 15 ml). The organic layer was dried over Na_2SO_4 and the solvent was removed under reduced pressure. The residue was purified by chromatography on alumina (neutral, activity 5, PE : CH_2Cl_2 2 : 1). The crude product was dissolved in CH_2Cl_2 and dropped into methyl *tert*-butyl ether. CH_2Cl_2 was removed under reduced pressure and the precipitate was filtered off and dried *in vacuo* which afforded 110 mg (69%) of a light red powder, mp 264 °C (Found: C, 82.32; H, 5.85; N, 12.17. Calc. for $C_{32}H_{26}N_4$: C, 82.38; H, 5.62; N, 12.01%); δ_H(250 MHz, [D_6]benzene) 7.02 (2 H, dd, $^4J_{HH}$ 1.53, $^3J_{HH}$ 7.93, arom. H), 6.72–6.63 (4 H, arom. H), 6.28 (2 H, d, $^4J_{HH}$ 1.53, arom. H), 6.10–5.99 (4 H, arom. H), 5.78 (2 H, d, $^3J_{HH}$ 8.25, arom. H), 2.30 (6 H, s, –CH_3), 2.27 (6 H, s, –CH_3); *m*/*z* 466 (M^+, 100%), 218 ($M^{2+} - 2\ CH_3$, 96%).

1,4-Bis[2-(5,10-dihydro-5,10-dimethylphenazinyl)ethynyl]-benzene 3. $Pd(PhCN)_2Cl_2$ (9.18 mg; 23.9 μmol), Cu(I)I (3.04 mg; 16.0 μmol), P(*t*-Bu)$_3$ (145 μl of a 0.33 M solution in hexane; 47.9 μmol), diisopropylamine (135 μl; 0.961 mmol), **10** (187 mg; 0.798 mmol) and 1,4-diiodobenzene (0.132 mg; 0.400 mmol) were dissolved in dioxane (1 ml) and stirred for 60 hours at RT. The solvent was removed *in vacuo*. The residue was purified by chromatography on alumina (neutral, activity 5, gradient PE ⟶ CH_2Cl_2). The crude product was dissolved in CH_2Cl_2 and dropped into methyl *tert*-butyl ether. CH_2Cl_2 was removed under reduced pressure and the precipitate was filtered off and dried *in vacuo* which afforded 188 mg (87%) of a light red powder, mp 261–262 °C (Found: C, 83.19; H, 5.50; N, 10.05. Calc. for $C_{38}H_{30}N_4$: C, 84.10; H, 5.57; N, 10.32%); δ_H(250 MHz, [D_6]benzene) 7.51 (4 H, s, phenylene), 6.94 (2 H, dd, $^4J_{HH}$ 1.53, $^3J_{HH}$ 7.95, arom. H), 6.76–6.71 (4 H, arom. H), 6.57 (2 H, d, $^4J_{HH}$ 1.53, arom. H), 6.54–6.45 (4 H, arom. H), 5.32 (2 H, d, $^3J_{HH}$ 7.95, arom. H), 3.00 (6 H, s, –CH_3), 2.99 (6 H, s, –CH_3);

m/z 542 (M^+, 83%), 256 (M^{2+} − 2 CH_3, 100%); MS (EI, 70 eV, high resolution): *m/z* found: 542.2470, calc. for $C_{38}H_{30}N_4$: 542.2471.

9,10-Bis[2-(5,10-dihydro-5,10-dimethylphenazinyl)ethynyl]-anthracene 4. $Pd(PhCN)_2Cl_2$ (6.14 mg; 16.0 μmol), Cu(I)I (2.03 mg; 10.7 μmol), P(*t*-Bu)$_3$ (97.1 μl of a 0.33 M solution in hexane; 32.0 μmol), diisopropylamine (90.1 μl; 0.641 mmol), **10** (125 mg; 0.534 mmol) and 9,10-dibromoanthracene (89.4 mg; 0.266 mmol) were dissolved in dioxane (1 ml) and stirred for 60 hours at RT. The solvent was removed *in vacuo*. The residue was purified by chromatography on alumina (neutral, activity 5, gradient PE : CH_2Cl_2 4 : 1 ⟶ CH_2Cl_2). The crude product was precipitated several times from a CH_2Cl_2 solution with methyl *tert*-butyl ether to give 134 mg (78%) of a dark violet powder, mp >300 °C; δ_H(250 MHz, [D_6]benzene) 9.10 (4 H, AA′, anthracene), 7.39 (4 H, BB′, anthracene), 6.97 (2 H, dd, $^4J_{HH}$ 1.53, $^3J_{HH}$ 8.23, arom. H), 6.77–6.69 (4 H, arom. H), 6.68 (2 H, d, $^4J_{HH}$ 1.53, arom. H), 6.15–6.08 (4 H, arom. H), 6.05 (2 H, d, $^3J_{HH}$ 8.23, arom. H), 2.41 (6 H, s, –CH_3), 2.41 (6 H, s, –CH_3); *m/z* 642 (M^+, 6%); MS (EI, 70 eV, high resolution): *m/z* found: 642.2799, calc. for $C_{46}H_{34}N_4$: 642.2784.

Electrochemistry

Cyclic voltammograms were measured with a computer controlled BAS CV50W potentiostat in dry and oxygen-free solvents (MeCN and benzonitrile) with 0.2 M tetrabutylammonium hexafluorophosphate and tetrabutylammonium tetrafluoroborate, respectively, as the supporting electrolyte and with ~0.001 M substrate under an argon inert gas atmosphere. A conventional three-electrode set-up was used with a platinum disk working electrode and a Ag/AgCl pseudo reference electrode. The redox potentials were referenced against internal ferrocene/ferrocenium (Fc/Fc^+). Digital simulation of the CVs for all compounds was done with DigiSim 3.03.[36]

UV/Vis/NIR-spectroscopy

UV/Vis/NIR spectra were recorded with a Jasco V-570 spectrometer. UV/Vis/NIR-spectroscopic measurements were done in dry and oxygen-free benzonitrile with a conventional 1 cm quartz cuvette. For chemical oxidation an $SbCl_5$ (1 M) acetonitrile solution was diluted with benzonitrile to 0.005 M. This solution was added drop by drop to a 10^{-5} M solution of $\mathbf{1}^+$–$\mathbf{5}^+$ in benzonitrile. After each drop a spectrum was recorded over the whole range (2500–250 nm) with a scan rate of 1000 nm min^{-1}. In order to minimise overlap of the spectra of the monocations with those of the dications, spectra at *ca.* one third of the maximal absorbance of the IV-CT bands were used for IV-CT band fits. These spectra were multiplied by the appropriate factor to yield the maximal IV-CT absorbance. The spectra obtained in that way were then corrected for the comproportionation equilibra using the redox potential splitting between first and second oxidation wave (see Table 3) according to the literature.[3,15]

Crystal data and structure determination for DHP

The data set was collected at low temperature using an oil-coated shock-cooled crystal[44–46] on a Bruker APEX-CCD diffractometer with Mo-Kα (λ = 71.073 pm) radiation equipped with a low temperature device at 173(2) K. The structure was solved by direct methods (SHELXS-NT 97)[47] and refined by full-matrix least squares methods against F^2 (SHELXL-NT 97).[48] *R* values defined as $R1 = \Sigma||F_o| - |F_c||/\Sigma|F_o|$, $wR2 = [\Sigma w(F_o^2 - F_c^2)^2/\Sigma w(F_o^2)^2]^{0.5}$, $w = [\sigma^2(F_o^2) + (g_1P)^2 + g_2P]^{-1}$, $P = 1/3[\max(F_o^2,0) + 2F_c^2]$. SADABS 2.0 was employed as a program for empirical absorption correction.[49] **DHP**: $C_{14}H_{14}N_2$, M = 210.27, hexagonal, space group $P6_3/m$ (no. 176), a = 13.178(6) Å, c = 11.091(5) Å, V = 1668.1(13) Å^3, Z = 6, $\rho_{cal.}$ = 1.256 Mg m^{-3}, μ = 0.075 mm^{-1}, $F(000)$ = 672. 4471 reflections measured, 1067 unique, R(int) = 0.0412, $wR2$ (all data) = 0.0968, $R1(I > 2\sigma(I))$ = 0.0342, g_1 = 0.0585, g_2 = 0.1316 for 1062 data, no restraints and 81 parameters. All non-hydrogen atoms were refined anisotropically. Selected bond lengths and angles of **DHP** can be found in Table 1 and Table 2. Crystallographic data for the structure of **DHP** are deposited at the Cambridge Crystallographic Data Centre. CCDC reference number 185376. See http://www.rsc.org/suppdata/p2/b2/b204392k/ for crystallographic files in .cif or other electronic format. Copies of the data can be obtained free of charge on application to CCDC, 12 Union Road, Cambridge, UK CB2 1EZ [Fax: (Internat.) +44-1223/336-033, E-mail: deposit@ccdc.cam.ac.uk].

Acknowledgements

This paper is dedicated to Professor Dr Dr h.c. Waldemar Adam on the occasion of his 65th birthday. We are grateful to the Fonds der Chemischen Industrie, the Deutsche Forschungsgemeinschaft (Graduiertenkolleg "Elektronendichte") and the Bayerisches Staatsministerium für Unterricht, Kultus, Wissenschaft und Kunst (FORMAT Project). We also acknowledge support by JASCO GmbH Deutschland.

References

1 S. F. Nelsen, *Chem. Eur. J.*, 2000, **6**, 581.
2 S. F. Nelsen, J. Adamus and J. J. Wolff, *J. Am. Chem. Soc.*, 1994, **116**, 1589.
3 J.-P. Launay, *Chem. Soc. Rev.*, 2001, **30**, 386.
4 J. Bonvoisin, J.-P. Launay, C. Rovira and J. Veciana, *Angew. Chem., Int. Ed. Engl.*, 1994, **33**, 2106.
5 C. Rovira, D. Ruiz-Molina, O. Elsner, J. Vidal-Gancedo, J. Bonvoisin, J.-P. Launay and J. Veciana, *Chem. Eur. J.*, 2001, **7**, 240.
6 S. F. Rak and L. L. Miller, *J. Am. Chem. Soc.*, 1992, **114**, 1388.
7 S. V. Lindeman, S. V. Rosokha, D. Sun and J. K. Kochi, *J. Am. Chem. Soc.*, 2002, **124**, 843.
8 S. F. Nelsen, D. A. Trieber, R. F. Ismagilov and Y. Teki, *J. Am. Chem. Soc.*, 2001, **123**, 5684.
9 S. F. Nelsen, R. F. Ismagilov, K. E. Gentile and D. R. Powell, *J. Am. Chem. Soc.*, 1999, **121**, 7108.
10 C. Lambert and G. Nöll, *J. Am. Chem. Soc.*, 1999, **121**, 8434.
11 S. F. Nelsen, G. Li and A. Konradsson, *Org. Lett.*, 2001, **3**, 1583.
12 J. Bonvoisin, J.-P. Launay, M. Van der Auweraer and F. C. De Schryver, *J. Phys. Chem.*, 1994, **98**, 5052.
13 J. Bonvoisin, J.-P. Launay, W. Verbouwe, M. Van der Auweraer and F. C. De Schryver, *J. Phys. Chem.*, 1996, **100**, 17079.
14 C. Lambert, W. Gaschler, E. Schmälzlin, K. Meerholz and C. Bräuchle, *J. Chem. Soc., Perkin Trans. 2*, 1999, 577.
15 C. Lambert and G. Nöll, *Angew. Chem., Int. Ed.*, 1998, **37**, 2107.
16 C. Lambert, G. Nöll and F. Hampel, *J. Phys. Chem. A*, 2001, **105**, 7751.
17 B. S. Brunschwig and N. Sutin, *Reflections on the Two-state Electron-transfer Model*, ed. V. Balzani, Wiley-VCH, Weinheim, 2001.
18 N. S. Hush, *Coord. Chem. Rev.*, 1985, **64**, 135.
19 S. F. Nelsen, H. Chang, J. J. Wolff and J. Adamus, *J. Am. Chem. Soc.*, 1993, **115**, 12276.
20 T. J. J. Müller, *Tetrahedron Lett.*, 1999, **40**, 6563.
21 R. Engel, PhD Thesis, Universität Regensburg, 1999.
22 R. J. Cave and M. D. Newton, *Chem. Phys. Lett.*, 1996, **249**, 15.
23 M. D. Newton, *Adv. Chem. Phys.*, 1999, **106**, 303.
24 S. F. Nelsen and M. D. Newton, *J. Phys. Chem. A*, 2000, **104**, 10023.
25 S. F. Nelsen and F. Blomgren, *J. Org. Chem.*, 2001, **66**, 6551.
26 R. A. Marcus, *J. Phys. Chem.*, 1989, **93**, 3078.
27 S. F. Nelsen, R. F. Ismagilov and D. A. Trieber, *Science*, 1997, **278**, 846.
28 I. G. M. Campbell, C. G. Le Fevre, R. J. W. Le Fevre and E. E. Turner, *J. Chem. Soc.*, 1938, 404.
29 Z. G. Soos, H. J. Keller, K. Ludolf, J. Queckboerner, D. Wehe and S. Flandrois, *J. Chem. Phys.*, 1981, **74**, 5287.
30 S. Jayanty, D. B. K. Kumar and T. P. Radhakrishnan, *Synth. Met.*, 2000, **114**, 37.
31 H. J. Keller, W. Moroni, D. Noethe, M. Scherz and J. Weiss, *Z. Naturforsch., B*, 1978, **33**, 838.
32 M. Malagoli and J. L. Brédas, *Chem. Phys. Lett.*, 2000, **327**, 13.

33 D. L. Vivian and J. L. Hartwell, *J. Org. Chem.*, 1953, **18**, 1065.
34 A. Sugimoto, T. Kotani, J. Tsujimoto and S. Yoneda, *J. Heterocycl. Chem.*, 1989, **26**, 435.
35 T. Hundertmark, A. F. Littke, S. L. Buchwald and G. C. Fu, *Org. Lett.*, 2000, **2**, 1729.
36 M. Rudolph and S. W. Feldberg, DigiSim 3.03a, Bioanalytical Systems, Inc., 1994–2000.
37 N. G. Connelly and W. E. Geiger, *Chem. Rev.*, 1996, 877.
38 F. Hilgers, W. Kaim, A. Schulz and S. Zalis, *J. Chem. Soc., Perkin Trans. 2*, 1994, 135.
39 S. F. Nelsen, R. F. Ismagilov and D. R. Powell, *J. Am. Chem. Soc.*, 1998, **120**, 1924.
40 C. Lambert, G. Nöll and J. Schelter, *Nat. Mater.*, 2002, **1**, in press.
41 R. J. Crutchley, *Adv. Inorg. Chem.*, 1994, **41**, 273.
42 R. J. Mortimer, *Electrochim. Acta*, 1999, **44**, 2971.
43 D. R. Rosseinsky and R. J. Mortimer, *Adv. Mater.*, 2001, **13**, 783.
44 T. Kottke and D. Stalke, *J. Appl. Crystallogr.*, 1993, **26**, 615.
45 T. Kottke, R. J. Lagow and D. Stalke, *J. Appl. Crystallogr.*, 1996, **29**, 465.
46 D. Stalke, *Chem. Soc. Rev.*, 1998, **27**, 171.
47 G. M. Sheldrick, *Acta Crystallogr., Sect. A*, 1990, **46**, 467.
48 G. M. Sheldrick, SHELXL-NT 97, Program for Crystal Structure Refinement, Universität Göttingen, 1997.
49 G. M. Sheldrick, Program for empirical absorption correction, Universität Göttingen, 2000.